

Temporal cavity soliton interaction in passively mode-locked semiconductor lasers

Andrei G. Vladimirov

Weierstrass Institute, Mohrenstr. 39, 10117 Berlin, Germany

Weak interaction of temporal cavity solitons due to gain saturation and recovery in a delay differential model of a long cavity semiconductor laser is studied numerically and analytically using an asymptotic approach. It is shown that in addition to the usual soliton repulsion leading to a harmonic mode-locking regimes a soliton attraction is also possible in a laser with nonzero linewidth enhancement factor. It is shown numerically that this attraction can lead either to a pulse merging or to a pulse bound state formation.

I. INTRODUCTION

Temporal cavity solitons (TCSs) are short nonlinear optical pulses generated by mode-locked lasers and optical microresonators and preserving their shape in the course of propagation [5, 8, 9]. In lasers, unlike the usual self-starting mode-locked pulses generated above the linear laser threshold, TCSs coexist with stable laser off regime and require a finite perturbation for their excitation. For example, when the cavity length of a laser with a semiconductor gain medium is sufficiently large, usual mode-locked pulses can be transformed into TCSs [13] corresponding to a non-self-starting mode-locking regime. In many practical situations when more than one TCSs are excited in an optical cavity weak interaction between the TCSs may take place via their exponentially decaying tails. Spatial and temporal dissipative soliton interaction in lasers with saturable absorbers was studied in many publications in the case when the gain and absorber populations were adiabatically eliminated and the interaction took place only via the overlapping electric fields of the pulses [1–3, 12, 22]. Less investigated is the interaction of mode-locked pulses in the presence of finite relaxation times of the gain and/or absorber media. In this case the electromagnetic field saturates gain and absorption behind the pulse and their slow relaxation can affect the position of the next pulse traveling in the cavity. This type of interaction was studied in Ref. [4, 11, 15, 17, 29]. In particular, it was demonstrated theoretically and verified experimentally with solid state and fiber lasers [11] that the interaction due to gain depletion and very slow recovery can produce a repulsive force between adjacent pulses leading to the formation of harmonic mode-locking regimes. Similar conclusion was made in Ref. [15] using the delay differential equation (DDE) model [25–27] of a mode-locked monolithic semiconductor laser, where similarly to Ref. [11] the gain recovery time was much longer than the cavity round trip time. Here using the same DDE model I consider the mode-locked pulse interaction in the TCS regime, where the cavity round trip time is sufficiently long, much longer than the gain recovery time. Basing on asymptotic approach the equations governing slow evolution of the time separation and phase difference of the interacting TCSs are derived and analyzed. Asymptotic study of weak TCS interaction in DDE models of optical systems

was already carried out earlier in [14, 16, 20]. However, only in Ref. [20] devoted to the TCS interaction in nonlinear mirror mode-locked laser and here a closed analytical form of the interaction equations is derived. Using these equations I show that the TCS interaction scenarios can be more rich than those described in [11, 15]. Apart from the pulse repulsion resulting in a harmonic mode-locking regime, TCS attraction leading either to pulse merging or bound state formation can take place in a laser with nonzero linewidth enhancement factor. Note, that soliton attraction leading to a bound state formation was observed earlier in Ref. [17] in a complex Ginzburg-Landau equation type mode-locked laser model with second order dispersion and in the DDE model of a nonlinear mirror mode-locked laser [20]. Note, however, that unlike the present work, in both those papers the Kerr nonlinearity played a decisive role in the process of the pulse formation. Furthermore, since Ref. [17] considers the limit of infinitely large gain recovery time, the mechanism of the pulse interaction in this paper was different and can be attributed to the saturation and slow recovery of the absorption, rather than the gain.

II. MODEL EQUATIONS

The DDE model of a passively mode-locked semiconductor laser for the electric field amplitude $A(t)$ at the entrance of the laser absorber section, saturable gain $G(t)$, and saturable absorption $Q(t)$ in the gain and absorber sections, respectively, can be written in the form [25–27]:

$$\gamma^{-1} \partial_t A + (1 + i\omega) A = R(t - T) A(t - T), \quad (1)$$

$$\partial_t G = g_0 - \gamma_g G - e^{-Q} (e^G - 1) |A|^2, \quad (2)$$

$$\partial_t Q = q_0 - \gamma_q Q - s (1 - e^{-Q}) |A|^2, \quad (3)$$

with

$$R(t) = \sqrt{\kappa} e^{(1 - i\alpha_g)G(t)/2 - (1 - i\alpha_q)Q(t)/2 + i\phi - i\omega T}.$$

Here t is the time variable, κ is the attenuation factor describing linear non-resonant intensity losses per cavity

round trip, α_g and α_q are the linewidth enhancement factors in the gain and absorber sections, respectively. The time delay parameter T stands for the cold cavity round trip time, γ is the spectral filtering bandwidth, γ_g and γ_q are the normalized carrier relaxation rates in the gain and absorber sections, and s is the ratio of the saturation intensities in these sections. The pump parameter g_0 depends on the injection current in the gain section, while q_0 is the unsaturated loss parameter, which depends on the inverse voltage applied to the absorber section. The parameter ϕ is the phase shift describing the detuning between the central frequency of the spectral filter and the closest cavity mode and ω the reference frequency.

It is well known that in a certain parameter domain Eqs. (1)-(3) demonstrate pulsed solutions corresponding to fundamental single pulse and harmonic multi-pulse mode-locking regimes [25–27]. Furthermore, it was shown in [13] that when the laser cavity is sufficiently long, so that the round trip time is much larger than the gain relaxation time, these pulses can be transformed into TCSs sitting on the stable laser off solution. In this situation two well separated mode-locking pulses can interact only weakly via their exponentially decaying tails. Furthermore, when the pulses are sufficiently far away from one another, this interaction is mainly due to the gain component G , which usually decays much slower than the electric field envelope A and the saturable absorption Q . Note, however, that when the distance between the TCSs becomes small enough the interaction via absorber component also might come into play and even lead to the pulse bound state formation, see Ref. [17], where the case of infinitely large gain recovery time was considered.

In order to derive the TCS interaction equations we rewrite the model equations in a more general real vector form

$$\partial_t \mathbf{U} = \mathbf{F}_\omega(\mathbf{U}) + \mathbf{H}_\omega[\mathbf{U}(t-T)], \quad (4)$$

where $\mathbf{U} = (U_1 \ U_2 \ U_3 \ U_4)^T$ is real column vector with $U_1 = \text{Re } A$, $U_2 = \text{Im } A$, $U_3 = G - g_0/\gamma_g$, $U_4 = Q - q_0/\gamma_q$,

$$\mathbf{F}_\omega(\mathbf{U}) = \begin{pmatrix} -\gamma(U_1 - \omega U_2) \\ -\gamma(U_2 + \omega U_1) \\ -\gamma_g U_3 - e^{-U_4 - Q_0} (e^{U_3 + G_0} - 1) (U_1^2 + U_2^2) \\ -\gamma_q U_4 - s(1 - e^{-U_4 - Q_0}) (U_1^2 + U_2^2) \end{pmatrix},$$

and

$$\mathbf{H}_\omega(\mathbf{U}) = \begin{pmatrix} -\text{Re}[R(U_1 + iU_2)] \\ -\text{Im}[R(U_1 + iU_2)] \\ 0 \\ 0 \end{pmatrix}$$

with

$$R(t) = \gamma\sqrt{\kappa}e^{(1-i\alpha_g)(U_3+g_0/\gamma_g)/2-(1-i\alpha_q)(U_4+q_0/\gamma_q)/2-i\omega T}.$$

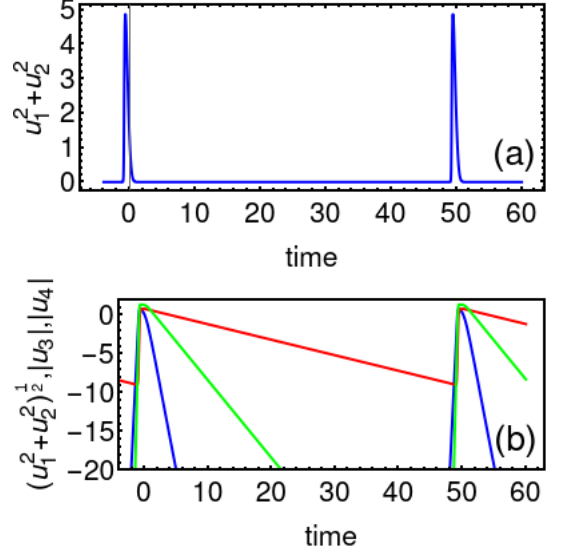


Figure 1. Intensity time trace of the periodic TCS solution of Eqs. (1)-(3) (a). Temporal evolution of the absolute values of the field envelope (blue), gain (red) and loss (green) components of the TCS solution in logarithmic scale (b). Parameters are: $\alpha_g = \alpha_q = 0$, $g_0 = 0.5$, $q_0 = 4.0$, $\kappa = 0.8$, $s = 10.0$, $\gamma = 5.0$, $\gamma_g = 0.2$, $\gamma_q = 1.0$, $T = 50.0$. The solution period is $T_0 = 50.138425$ and $\omega_0 = 0$.

III. TEMPORAL CAVITY SOLITON

Let us assume that the inequalities

$$\gamma^{-1} < \gamma_q^{-1} < \gamma_g^{-1} \ll T, \quad (5)$$

for the relaxation rates in the model equations (1)-(3) are satisfied. This means that the round trip time in a multimode semiconductor laser cavity is sufficiently long, much longer than the gain relaxation time. In this case the DDE model can have TCS solutions [13]. We will assume that such a solution corresponding to a narrow mode-locked pulse with the duration $\tau_p \sim \gamma^{-1}$ exists in a certain parameter domain and is given by $\omega = \omega_0$ and $\mathbf{U} = \mathbf{u} = (u_1 \ u_2 \ u_3 \ u_4)^T$ in terms of Eq. (4). Here $\mathbf{u}(t) = \mathbf{u}(t+T_0)$ is periodic in time with the period T_0 close to the delay time T . In terms of the original model equations (1)-(3) we have $\mathbf{u} = [\text{Re } A_0(t) \ \text{Im } A_0(t) \ G_0(t) - g_0/\gamma_g \ Q_0(t) - q_0/\gamma_q]^T$, where $A_0(t)$, $G_0(t)$, and $Q_0(t)$ is a T_0 -periodic TCS solution of these equations. Numerically calculated intensity time trace of the TCS solution is shown in Fig. 1(a).

The decay rates of the TCS tails are determined by the following linearization [18, 23, 28] of the model equations (1)-(3), on the trivial solution:

$$\gamma^{-1} \partial_t a + (1 + i\omega_0) a = R_0 a(t + \delta), \quad (6)$$

$$\partial_t v_3 = -\gamma_g v_3. \quad (7)$$

$$\partial_t v_4 = -\gamma_q v_4. \quad (8)$$

where $\mathbf{a} = v_1 + iv_2$, $\mathbf{v} = (v_1 \ v_2 \ v_2 \ v_4)^T$ is a small perturbations vector,

$$R_0 = \sqrt{\kappa} e^{(1-i\alpha_g)g_0/(2\gamma_g) - (1-i\alpha_q)q_0/(2\gamma_q) + i\phi + i\omega_0\delta},$$

and the time advance parameter is $\delta = T_0 - T$. It follows from Eqs. (7) and (8) that the decay rates of the TCS gain and absorber components at large positive times t are determined by the corresponding eigenvalues $\lambda_{g,q} = -\gamma_{g,q}$, while Eq. (6) has an infinite number of eigenvalues defined by

$$\lambda_k = -\gamma(1 + i\omega_0) - \delta^{-1} W_k \left[-\gamma\delta e^{-(1+i\omega_0)\gamma\delta} R_0 \right]. \quad (9)$$

where W_k is the Lambert function with the index $k = 0, \pm 1, \pm 2, \dots$. For the parameter values of Fig. 1 we get $\lambda_0 = -3.741$ and $\lambda_{-1} = 16.892$, while all other eigenvalues are complex and have positive real parts greater than λ_{-1} .

Assuming that the origin of the time coordinate, $t = 0$, is located at the TCS power peak we get from (7)-(9) that for $t > 0$ far away from the TCS core its trailing edge can be expressed as

$$u_{1,2} \sim b_{1,2} e^{\lambda_0 t}, \quad u_3 \sim b_3 e^{-\gamma_g t}, \quad u_4 \sim b_4 e^{-\gamma_q t}, \quad (10)$$

where $b_{1,2,3,4}$ are real constants that can be calculated numerically for given parameter values of Eqs. (1)-(3).

Next, let us consider the leading tail of the TCS at negative times, $t < 0$. Since Eqs. (7) and (8) have no eigenvalues with positive real parts, gain and absorber components of the TCS leading edge, u_3 and u_4 decay faster than exponentially in negative time [23]. The field component $u_1 + iu_2$ of the leading tail decays exponentially at $t < 0$ with the decay rate determined by the eigenvalue λ_{-1} having smallest positive real part. Since the inequality $\gamma_{g,q} < |\lambda_0| < \lambda_{-1}$ is satisfied, the field component of the TCS decays faster in both time directions than the gain and absorber components in positive time. This means that the interaction via the electromagnetic field component can be neglected when considering the interaction of two well separated TCSs. Such type of interaction is typical of lasers with slow gain and absorption and can be viewed as the long-range interaction [20] unlike the short range interaction via overlapping electric fields considered in [2, 3, 12, 19, 22]. Furthermore, since gain and absorber components of a TCS decay faster than exponentially in negative time, the leading tails of the TCSs can be neglected in the derivation of the interaction equations. Figure 1(b) shows the time evolution of the absolute values of field envelope $\sqrt{U_{01}^2 + U_{02}^2}$, gain $|U_{03}|$, and absorption $|U_{04}|$ components of this solution in logarithmic scale. It is seen from this figure that the gain component dominates over the field and absorption ones during almost all the time interval between the two consequent pulses.

Linear stability of the TCS is determined by linearizing Eq. (4) at the solution $\mathbf{U} = \mathbf{u}$ and calculating the spectrum of the resulting linear operator \mathcal{L} . Due to the translational and phase shift symmetries of the model equations (1)-(3), $\mathbf{U}(t) \rightarrow \mathbf{U}(t - t_0)$ and $U_1 + iU_2 \rightarrow (U_1 + iU_2) e^{i\phi_0}$ with arbitrary constants t_0 and ϕ_0 , the operator \mathcal{L} has a pair of zero eigenvalues corresponding to the neutral (Goldstone) modes given by $\boldsymbol{\theta} = \partial_t \mathbf{u}$ and $\boldsymbol{\varphi} = (-u_2 \ u_1 \ 0 \ 0)^T$, respectively, $\mathcal{L}\boldsymbol{\theta} = -\partial_t \boldsymbol{\theta} + \mathcal{B}(\mathbf{u})\boldsymbol{\theta} + \mathcal{C}[\mathbf{u}(t - T)]\boldsymbol{\theta}^\dagger(t - T) = 0$, where $\mathcal{B}(\mathbf{u}) [(\mathcal{C}(\mathbf{u}))]$ is the linearization matrix of $\mathbf{F}_{\omega_0}(\mathbf{U}) [\mathbf{H}_{\omega_0}(\mathbf{U})]$ at $\mathbf{U} = \mathbf{u}$ and $\mathcal{L}\boldsymbol{\varphi} = 0$. Let us assume that the TCS is stable, which means that the rest of the spectrum of the operator \mathcal{L} lies in the left half of the complex plane. Similarly, the linear operator \mathcal{L}^\dagger adjoint to \mathcal{L} has a pair of zero eigenvalues associated with the so-called adjoint neutral modes $\boldsymbol{\theta}^\dagger$ and $\boldsymbol{\varphi}^\dagger$, $\mathcal{L}^\dagger \boldsymbol{\theta}^\dagger = \partial_t \boldsymbol{\theta}^\dagger + \boldsymbol{\theta}^\dagger \mathcal{B}(\mathbf{u}) + \boldsymbol{\theta}^\dagger(t + T)\mathcal{C}(\mathbf{u}) = 0$ and $\mathcal{L}^\dagger \boldsymbol{\varphi}^\dagger = 0$. The adjoint neutral modes are assumed to be biorthogonal to the neutral modes, $\langle \boldsymbol{\theta}^\dagger \cdot \boldsymbol{\varphi} \rangle = \langle \boldsymbol{\varphi}^\dagger \cdot \boldsymbol{\theta} \rangle = 0$ and $\langle \boldsymbol{\theta}^\dagger \cdot \boldsymbol{\theta} \rangle = \langle \boldsymbol{\varphi}^\dagger \cdot \boldsymbol{\varphi} \rangle = 1$, where $\langle \mathbf{x}^\dagger \cdot \mathbf{y} \rangle = \int_0^{\tau_0} \mathbf{x}^\dagger \cdot \mathbf{y} dt$. Since the adjoint operator \mathcal{L}^\dagger is obtained from \mathcal{L} by the transformations including the time reversal, $t \rightarrow -t$, the asymptotic behavior of the row vector adjoint neutral modes $\boldsymbol{\theta}^\dagger = (\theta_1^\dagger \ \theta_2^\dagger \ \theta_3^\dagger \ \theta_4^\dagger)$ and $\boldsymbol{\varphi}^\dagger = (\varphi_1^\dagger \ \varphi_2^\dagger \ \varphi_3^\dagger \ \varphi_4^\dagger)$ at sufficiently large negative times $t < 0$ is given by

$$\theta_{1,2}^\dagger \sim c_{1,2} e^{-\lambda_0 t}, \quad \theta_3^\dagger \sim c_3 e^{\gamma_g t}, \quad \theta_4^\dagger \sim c_4 e^{\gamma_q t}, \quad (11)$$

$$\varphi_{1,2}^\dagger \sim d_{1,2} e^{-\lambda_0 t}, \quad \varphi_3^\dagger \sim d_3 e^{\gamma_g t}, \quad \varphi_4^\dagger \sim d_4 e^{\gamma_q t}, \quad (12)$$

where $c_{1,2,3,4}$ and $d_{1,2,3,4}$ are real coefficients, which can be calculated numerically. Similarly to the leading tail of the TCS solution, the trailing tail of the gain and absorber components of the adjoint neutral modes decay faster than exponentially at $t > 0$. Therefore, trailing tails of the adjoint neutral modes will be neglected when deriving the TCS interaction equations. The temporal evolution of the field, gain, and loss components of the translational adjoint neutral mode $\boldsymbol{\theta}^\dagger = (\theta_1^\dagger \ \theta_2^\dagger \ \theta_3^\dagger \ \theta_4^\dagger)$ are shown in Fig. 2. We see that similarly to Fig. 1 the gain component θ_3^\dagger of the adjoint neutral mode dominates almost everywhere between the consequent mode-locked pulses. Therefore, one can conclude that the pulse interaction via the field and absorber components can be neglected for the parameter values of these figures.

IV. INTERACTION EQUATIONS

To derive the equations describing slow evolution of the time coordinates and phases of weakly interacting TCSs we look for the solution of Eq. (4) in the form of a sum of two unperturbed TCS solutions plus a small correction

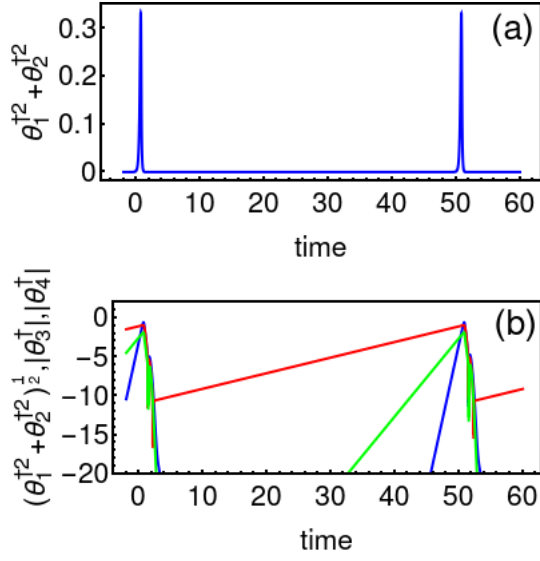


Figure 2. Intensity time trace of the adjoint neutral mode θ^\dagger as a function of time (a). Temporal evolution of the absolute values of the field (blue), gain (red), and loss (green) components of the translational adjoint neutral mode θ^\dagger in logarithmic scale (b). Parameters are the same as in Fig. 1.

$\mathbf{w}(\mathbf{t}) = \mathcal{O}(\epsilon)$ due to the interaction:

$$\mathbf{U} = \sum_{k=1}^2 \mathbf{u}_k + \mathbf{w}, \quad (13)$$

where $\mathbf{u}_k = (u_{1k} \ u_{2k} \ u_{3k} \ u_{4k})^T$ with $u_{1k} + iu_{2k} = [u_1(t - \tau_k) + iu_2(t - \tau_k)] e^{-i\phi_k}$, $u_{3k} = u_3(t - \tau_k)$, and $u_{4k} = u_4(t - \tau_k)$. Coordinates τ_k and phases ϕ_k of the interacting TCSs are assumed to be slow functions of time, $\partial_t \tau_k, \partial_t \phi_k = \mathcal{O}(\epsilon)$, $k = 1, 2$. The small parameter ϵ characterizes weak overlap of the TCSs. Similarly to the case of dissipative soliton interaction in partial differential equation laser models [19, 21, 22, 24], the right hand side of the interaction equations, obtained for our DDE model can be expressed in terms of the TCS solutions and their adjoint neutral modes evaluated at the point between the two TCSs [20]. The details of the calculations are given in the Appendix A, where it is shown that the interaction equations for the time separation $\Delta\tau = \tau_2 - \tau_1$ and phase difference $\Delta\phi = \phi_2 - \phi_1$ of a pair of interacting T_0 -periodic TCS take the form

$$\partial_t \Delta\tau \approx \theta_1^\dagger(T_0/2) \mathbf{u}_2(T_0/2) - \theta_2^\dagger(0) \mathbf{u}_1(0), \quad (14)$$

$$\partial_t \Delta\phi \approx \varphi_1^\dagger(T_0/2) \mathbf{u}_2(T_0/2) - \varphi_2^\dagger(0) \mathbf{u}_1(0), \quad (15)$$

where $\theta_k^\dagger = \theta^\dagger(t - t_k)$ and $\varphi_k^\dagger = \varphi^\dagger(t - t_k)$ are the adjoint neutral modes evaluated at the k th TCS ($k = 1, 2$) and without the loss of generality one can assume that $t = 0$ and $t = T_0/2$ correspond, respectively, to the middle point between the two interacting TCSs and the opposite point on a circle with the circumference T_0 .

Substituting asymptotic expressions (10), (11), and (12) into the interaction equations (14) and (15) and neglecting the field components gives

$$\partial_t \Delta\tau = K_{\tau g} \left[e^{-\gamma_g(T_0 - \Delta\tau)} - e^{-\gamma_g \Delta\tau} \right] \quad (16)$$

$$+ K_{\tau q} \left[e^{-\gamma_q(T_0 - \Delta\tau)} - e^{-\gamma_q \Delta\tau} \right], \quad (17)$$

$$\partial_t \Delta\phi = K_{\phi g} \left[e^{-\gamma_g(T_0 - \Delta\tau)} - e^{-\gamma_g \Delta\tau} \right] \quad (18)$$

$$+ K_{\phi q} \left[e^{-\gamma_q(T_0 - \Delta\tau)} - e^{-\gamma_q \Delta\tau} \right] \quad (19)$$

with $K_{\tau g} = b_3 c_3$, $K_{\tau q} = b_4 c_4$, $K_{\phi g} = b_3 d_3$, and $K_{\phi q} = b_4 d_4$. Interaction equations (17) and (19) describe the long-range interaction of two well separated TCS via their gain and absorber components and do not take into account the short range interaction via weakly overlapping electric field envelopes of the TCSs. They reflect the fact that in a ring cavity the interaction of the two TCSs is twofold. The trailing tail of the first (second) TCS overlaps with the leading tail of the adjoint neutral mode of the second (first) TCS which is located by $\Delta\tau$ ($T_0 - \Delta\tau$) behind it. This is reflected by the presence of the two exponential terms in the square brackets of Eqs. (17) and (19). As it was already noted above, due to the inequality $\gamma_q > \gamma_g$ typical of semiconductor lasers, the interaction force related to the absorber component decays much faster than that due to the gain component and the terms proportional to $K_{\tau q}$ and $K_{\phi q}$ can be neglected in the interaction equations. In the case of TCS repulsion ($K_{\tau g} < 0$) such type of twofold interaction leads to a regime with two equally spaced pulses per cavity round trip corresponding to a harmonic mode-locking regime.

V. RESULTS OF NUMERICAL SIMULATIONS

For the parameter values of Figs. 1 and 2 corresponding to zero linewidth enhancement factors, $\alpha_g = \alpha_q = 0$, numerically we get $K_{\tau g} = -1.120$ and $K_{\tau q} = 2.145$ in Eq. (17), while the second interaction equation (19) transforms into $\partial_t \Delta\phi = 0$ due to the relation $K_{\phi g} = K_{\phi q} = d_3 = d_4 = 0$, which is the consequence of $\omega_0 = \text{Im} A_0 = 0$. Negative value of $K_{\tau g}$ means that the TCS interaction is repulsive, while positive $K_{\tau q}$ corresponds to TCS attraction via the absorber component. For the parameter values of these figures, however, the interaction via gain component dominates for almost all sufficiently large soliton separations, as it was discussed above, and the soliton attraction due to the absorber component is hardly possible to observe. This is illustrated in Fig. 3 where the soliton repulsion is illustrated by numerical integration of Eqs. (1)-(3) using the RADAR5 code [6]. The initial condition was taken as a sum of two or more well separated unperturbed TCSs. Figure 3(a) shows the standard mechanism of the harmonic mode-locking regime formation as a result of the repulsion of a pair of TCSs due to the interaction via the gain component. Figure 3(b)

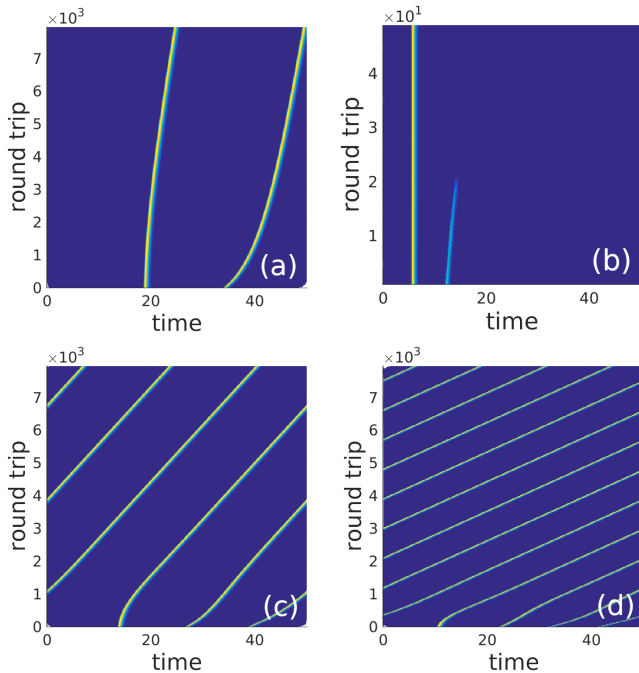


Figure 3. TSC repulsion due to the interaction via the gain component leading to a harmonic mode-locking regimes with two (a) and three (c) and four (d) pulses per cavity round trip. Panel (b) illustrates repulsive interaction resulting in the annihilation of the second pulse. (a), (b), and (c) - $g_0 = 0.5$. (d) - $g_0 = 0.8$. Other parameters the same as in Fig. 1.

was obtained for the same parameter values but with smaller initial separation of the two TCSs. It is seen that during the first stage of the interaction there is still repulsion between the TCSs, but later the second TCS loses energy and disappears. The equation $\partial_t \Delta\phi = 0$ means that the TCS phase difference remains almost constant in the course of the interaction. This difference is affected only by a very weak overlap of the field components which are neglected in the derivation of the interaction equations (17) and (19). Repulsive interaction of three and four TCSs leading to the development of harmonic mode-locking regimes with three and four pulses per cavity round trip are illustrated in Fig. 3(c) and 3(d), respectively.

The dependence of the interaction coefficient $K_{\tau g}$ on the linewidth enhancement factor α_g in the gain section is shown in Fig. 4(a). It is seen that this dependence is non-monotonous and has a pronounced resonant character. The interaction coefficient is negative (TCS repulsion) when the linewidth enhancement factor is sufficiently small, and it becomes positive (TCS attraction) with the increase of α_g showing a sharp peak around $\alpha_g \approx 0.94$. Further increase of the α_g leads to a non-monotonous gradual decrease of the interaction coefficient which becomes negative again at $\alpha_g \gtrsim 2.37$. Numerical simulation of the TCS interaction of Eqs. (1)-(3) with $\alpha_g = 2.0$, which corresponds to a small positive val-

ues of the interaction coefficient, is illustrated in Fig. 5. It is seen that the interaction is very asymmetric, see Refs. [4, 20, 21] and Appendix A. Figure 5(b) corresponding to $q_0 = 4.0$ and positive $K_{\tau g} \approx 0.854 \times 10^{-2}$ shows the TCS attraction leading to the merging of two pulses when one of them is annihilated after the collision. In Fig. 5(a) obtained for $q_0 = 5.0$ and $K_{\tau g} \approx 1.076 \times 10^{-2}$ the soliton attraction leads to a formation of a pulse bound state. Since for $\alpha_g \neq 0$ the relation $d_3 = d_4 = 0$ does not hold any more the TCS phases are evolving with round trip number in the course of interaction. Therefore, the bound state shown in Fig. 5(a) is similar to the “incoherent” bound state described in [20] with the phase difference $\Delta\phi$ between two pulses growing monotonously in time, see Fig. 6 illustrating the intensity time trace and the evolution of the TCS phase difference of the incoherent bound state. It was demonstrated in [20] that due to the electric field overlap of the interacting TCS such type of bound states is characterized by slightly oscillating time separation $\Delta\tau$. However, since the interaction via electric fields is extremely small for the bound state shown in Fig. 5(a) such oscillation is hardly possible to detect. Figure 4(b) shows the evolution of the inter-soliton time separation $\Delta\tau$ as a function of the round trip number obtained by direct numerical simulation of the laser model (1)-(3). The parameter values are the same as in Fig. 4(a). It is seen that for $\alpha_g = 0.5$ when the interaction coefficient $K_{\tau g}$ is negative the TCS interaction is repulsive leading to a harmonic mode-locking regime. On the contrary, for $\alpha_g = 1.0, 1.5, 2.0$, which correspond to $K_{\tau g} > 0$, the interaction results in the formation of a pulse bound states. Furthermore, comparing Fig. 4(b) with Fig. 4(a) we see that the smaller the interaction coefficient the weaker is the interaction force and, hence, the longer is the transient time before the equilibrium inter-pulse time separation is achieved. The final inter-pulse distance in the bound state is, however, only weakly dependent on the α_g and $K_{\tau g}$. Note, that the time separation of the pulses in the incoherent bound state shown in Fig. 5(a) is of the same order of magnitude as the gain relaxation time. This is why 6(a) the pulses in this bound state have significantly different peak powers [see Fig. 6(a)] and cannot any more be considered as individual TCSs. Therefore, the interaction equations (17) and (19) are not valid any more when the pulses are so close to one another. Indeed, in order the bound state to be formed, the attraction predicted by the interaction equations should be compensated by a repulsion at sufficiently small inter-pulse distances. This repulsion dominating at small pulse separations might be related to that in a laser with the cavity round trip time shorter or much shorter than the gain relaxation time discussed in [11, 15].

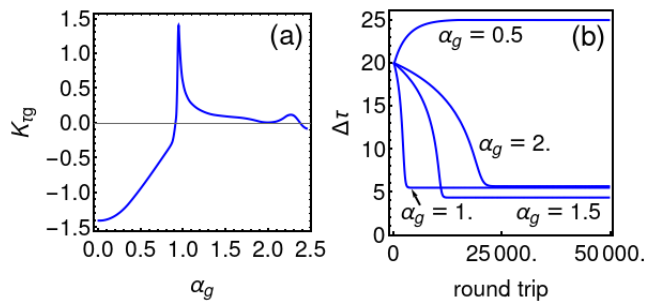


Figure 4. Interaction coefficient $K_{\tau g}$ as a function of α_g (a) and pulse time separation as a function of the round trip number (b). $g_0 = 0.8$. Other parameters are the same as in Fig. 1

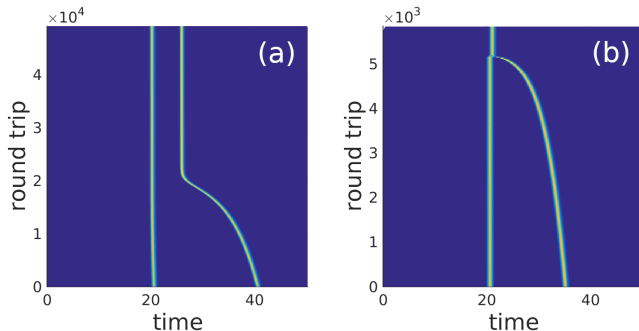


Figure 5. TCS interaction resulting in pulse bound state formation at $q_0 = 5.0$ (a) and pulse merging at $q_0 = 4.0$ (b). $g_0 = 0.8, \alpha_g = 2.0, \alpha_q = 0$. Other parameters are as in Fig. 3

VI. CONCLUSION

To conclude, using the DDE model interaction of two well separated TCSs in a long cavity mode-locked semiconductor laser was studied numerically and analytically. Interaction equations governing the slow evolution of the time separation and phase difference of the TCSs were derived and analyzed. Analytical results were compared

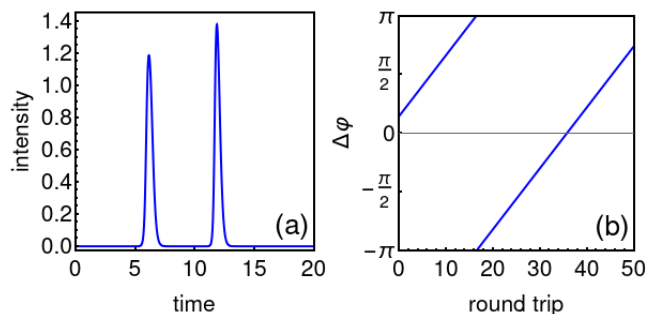


Figure 6. Intensity time-trace (a) and pulse phase difference (b) of the TCS bound state. Parameters are the same as in Fig. 5 (a).

to direct numerical simulations of the DDE mode-locking model. It was demonstrated that in addition to usual pulse repulsion predicted in [11, 15] an attractive TCS interaction is also possible in a laser with nonzero linewidth enhancement factor. This attractive interaction can result either in pulse merging or in a formation of incoherent pulse bound state. In the latter case the repulsion force counteracting the soliton attraction might be attributed to the standard mechanism of the mode-locking pulse repulsion described in [11, 15], which acts beyond the TCS limit. Incoherent bound pulse state discussed here is similar to that observed experimentally [10] and described theoretically [20] in a nonlinear mirror mode-locked laser. It also has a similarity to the “type A” pulse bound states reported in [17]. The mechanism of the latter bound states formation is, however, different from that described here and can be related to the TCS attraction due to the interaction via absorber component of the pulsed solution in a laser with infinitely large gain relaxation time.

ACKNOWLEDGMENTS

The support by the Deutsche Forschungsgemeinschaft (DFG projects No. 445430311 and No. 491234846) is gratefully acknowledged.

Appendix A: Derivation of the interaction equations

Substituting Eq. (13) into Eq. (4), collecting the first order terms in small parameter ϵ , and applying solvability conditions [7] to the resulting equation yield

$$\partial_t \tau_k = - \langle \boldsymbol{\theta}_k^\dagger \cdot \mathbf{P} \rangle, \quad \partial_t \phi_k = - \langle \boldsymbol{\varphi}_k^\dagger \cdot \mathbf{P} \rangle, \quad (\text{A1})$$

$$\mathbf{P} = - \partial_t \mathbf{u}_\Sigma + \mathbf{F}_{\omega_0}(\mathbf{u}_\Sigma) + \mathbf{H}_{\omega_0}[\mathbf{u}_\Sigma(t - T)], \quad (\text{A2})$$

where $\mathbf{u}_\Sigma = \mathbf{u}_1 + \mathbf{u}_2$, $\langle \cdot \rangle = \int_0^{T_0} \cdot dt$, and $\boldsymbol{\theta}_k^\dagger$ ($\boldsymbol{\varphi}_k^\dagger$) is the adjoint translational (phase) neutral mode evaluated the k th TCS, $k = 1, 2$.

Since \mathbf{u}_k is the solution of Eq. (4) the equality $\sum_{k=1}^2 \{-\partial_t \mathbf{u}_k + \mathbf{F}_{\omega_0}(\mathbf{u}_k) + \mathbf{H}_{\omega_0}[\mathbf{u}_k(t - T)]\} = 0$ is satisfied. Subtracting this equality from (A2) we get

$$\begin{aligned} \mathbf{P} = & \mathbf{F}_{\omega_0}(\mathbf{u}_\Sigma) - \sum_{k=1}^2 \mathbf{F}_{\omega_0}(\mathbf{u}_k) + \mathbf{H}_{\omega_0}[\mathbf{u}_\Sigma(t - \tau)] \\ & - \sum_{k=1}^2 \mathbf{H}_{\omega_0}[\mathbf{u}_k(t - T)]. \end{aligned} \quad (\text{A3})$$

Therefore, the equation for τ_2 in (A1) is

$$\begin{aligned} \partial_t \tau_2 = & - \langle \boldsymbol{\theta}_2^\dagger \cdot \mathbf{P} \rangle = - \langle \boldsymbol{\theta}_2^\dagger \cdot \left\{ \mathbf{F}_{\omega_0}(\mathbf{u}_\Sigma) - \sum_{k=1}^2 \mathbf{F}_{\omega_0}(\mathbf{u}_k) \right. \\ & \left. + \mathbf{H}_{\omega_0}[\mathbf{u}_\Sigma(t - T)] - \sum_{k=1}^2 \mathbf{H}_{\omega_0}[\mathbf{u}_k(t - T)] \right\} \rangle. \end{aligned} \quad (\text{A4})$$

Using T_0 -periodicity of $\boldsymbol{\theta}_2^\dagger$ and $\mathbf{u}_{1,2}$ Eq. (A4) can be rewritten as

$$\begin{aligned} \partial_t \tau_2 = & - \left\langle \boldsymbol{\theta}_2^\dagger \cdot \left[\mathbf{F}_{\omega_0}(\mathbf{u}_\Sigma) - \sum_{k=1}^2 \mathbf{F}_{\omega_0}(\mathbf{u}_k) \right] \right\rangle \\ & - \left\langle \boldsymbol{\theta}_2^\dagger(t+T) \cdot \left[\mathbf{H}_{\omega_0}(\mathbf{u}_\Sigma) - \sum_{k=1}^2 \mathbf{H}_{\omega_0}(\mathbf{u}_k) \right] \right\rangle. \end{aligned} \quad (\text{A5})$$

Next we split the integral $\langle \cdot \rangle = \int_0^{T_0} \cdot dt$ into two parts $\langle \cdot \rangle = \langle \cdot \rangle_1 + \langle \cdot \rangle_2$, where $\langle \cdot \rangle_1 = \int_{-T_0/2}^0 \cdot dt$ and $\langle \cdot \rangle_2 = \int_0^{T_0/2} \cdot dt$ are the integrals over the intervals $[-T_0/2, 0]$ and $[0, T_0/2]$, respectively:

$$\begin{aligned} \partial_t \tau_2 = & - \sum_{j=1}^2 \left\langle \boldsymbol{\theta}_2^\dagger \cdot \left[\mathbf{F}_{\omega_0}(\mathbf{u}_\Sigma) - \sum_{k=1}^2 \mathbf{F}_{\omega_0}(\mathbf{u}_k) \right] \right\rangle_j \\ & - \sum_{j=1}^2 \left\langle \boldsymbol{\theta}_2^\dagger(t+T) \cdot \left[\mathbf{H}_{\omega_0}(\mathbf{u}_\Sigma) - \sum_{k=1}^2 \mathbf{H}_{\omega_0}(\mathbf{u}_k) \right] \right\rangle_j. \end{aligned}$$

On the first interval $[-T_0/2, 0]$, where \mathbf{u}_2 is small, one obtains

$$\begin{aligned} \mathbf{F}_{\omega_0}(\mathbf{u}_\Sigma) - \mathbf{F}_{\omega_0}(\mathbf{u}_1) & \approx \mathcal{B}_1 \mathbf{u}_2, \\ \mathbf{H}_{\omega_0}(\mathbf{u}_\Sigma) - \mathbf{H}_{\omega_0}(\mathbf{u}_1) & \approx \mathcal{C}_1 \mathbf{u}_2, \end{aligned}$$

and

$$\mathbf{F}_{\omega_0}(\mathbf{u}_2) \approx \mathcal{B}_0 \mathbf{u}_2, \quad \mathbf{H}_{\omega_0}(\mathbf{u}_2) \approx \mathcal{C}_0 \mathbf{u}_2$$

with $\mathcal{B}_1 = \mathcal{B}(\mathbf{u}_1)$, $\mathcal{C}_1 = \mathcal{C}(\mathbf{u}_1)$ [$\mathcal{B}_0 = \mathcal{B}(0)$, and $\mathcal{C}_0 = \mathcal{C}(0)$] are the linearization matrices of $\mathbf{F}_{\omega_0}(\mathbf{U})$ and $\mathbf{H}_{\omega_0}(\mathbf{U})$ at $\mathbf{U} = \mathbf{u}_1$ ($\mathbf{U} = 0$). Similarly, on the second interval $[0, T_0/2]$, where \mathbf{u}_1 is small, one gets

$$\begin{aligned} \mathbf{F}_{\omega_0}(\mathbf{u}_\Sigma) - \mathbf{F}_{\omega_0}(\mathbf{u}_2) & \approx \mathcal{B}_2 \mathbf{u}_1, \\ \mathbf{H}_{\omega_0}(\mathbf{u}_\Sigma) - \mathbf{H}_{\omega_0}(\mathbf{u}_2) & \approx \mathcal{C}_2 \mathbf{u}_1, \end{aligned}$$

where $\mathcal{B}_2 = \mathcal{B}(\mathbf{u}_2)$ and $\mathcal{C}_2 = \mathcal{C}(\mathbf{u}_2)$ and

$$\mathbf{F}_{\omega_0}(\mathbf{u}_1) \approx \mathcal{B}_0 \mathbf{u}_1, \quad \mathbf{H}_{\omega_0}(\mathbf{u}_2) \approx \mathcal{C}_0 \mathbf{u}_1. \quad (\text{A6})$$

Hence, one obtains

$$\begin{aligned} \partial_t \tau_2 \approx & - \left\langle \boldsymbol{\theta}_2^\dagger \cdot (\mathcal{B}_1 - \mathcal{B}_0) \mathbf{u}_2 \right\rangle_1 \\ & - \left\langle \boldsymbol{\theta}_2^\dagger(t+T) \cdot (\mathcal{C}_1 - \mathcal{C}_0) \mathbf{u}_2 \right\rangle_1 \\ & - \left\langle \boldsymbol{\theta}_2^\dagger \cdot \{(\mathcal{B}_2 - \mathcal{B}_0) \mathbf{u}_1\} \right\rangle_2 \\ & - \left\langle \boldsymbol{\theta}_2^\dagger(t+T) \cdot (\mathcal{C}_2 - \mathcal{C}_0) \mathbf{u}_1 \right\rangle_2, \end{aligned}$$

where the first two terms in the right hand side containing the product of two small quantities $\boldsymbol{\theta}_2^\dagger$ and \mathbf{u}_2 on the first interval $[-T_0/2, 0]$ can be neglected. Thus one obtains

$$\begin{aligned} \partial_t \tau_2 \approx & - \left\langle \boldsymbol{\theta}_2^\dagger \cdot (\mathcal{B}_2 - \mathcal{B}_0) \mathbf{u}_1 \right\rangle_2 \\ & - \left\langle \boldsymbol{\theta}_2^\dagger(t+T) \cdot (\mathcal{C}_2 - \mathcal{C}_0) \mathbf{u}_1 \right\rangle_2. \end{aligned} \quad (\text{A7})$$

Since \mathbf{u}_1 is the solution of Eq. (4) it satisfies the equation $-\partial_t \mathbf{u}_1 + \mathbf{F}_{\omega_0}(\mathbf{u}_1) + \mathbf{H}_{\omega_0}(\mathbf{u}_2) = 0$. Using the relations (A6) valid on the second interval $[0, T_0/2]$ it can be rewritten on this interval in the form

$$-\partial_t \mathbf{u}_1 + \mathcal{B}_0 \mathbf{u}_1 + \mathcal{C}_0 \mathbf{u}_1(t-T) \approx 0. \quad (\text{A8})$$

The adjoint neutral mode $\boldsymbol{\theta}_2^\dagger$ satisfies the equation

$$\partial_t \boldsymbol{\theta}_2^\dagger + \boldsymbol{\theta}_2^\dagger \mathcal{B}_2 + \boldsymbol{\theta}_2^\dagger(t+T) \mathcal{C}_2 = 0. \quad (\text{A9})$$

Multiplying Eq. (A9) by \mathbf{u}_1 , subtracting from the resulting equation $\boldsymbol{\theta}_2^\dagger$ multiplied by Eq. (A8) and integrating over the second interval $[0, T_0/2]$ yields

$$\begin{aligned} \left\langle \boldsymbol{\theta}_2^\dagger \cdot (\mathcal{B}_2 - \mathcal{B}_0) \mathbf{u}_1 \right\rangle_2 & \approx - \left\langle \partial_t \boldsymbol{\theta}_2^\dagger \cdot \mathbf{u}_1 + \boldsymbol{\theta}_2^\dagger \cdot \partial_t \mathbf{u}_1 \right\rangle_2 \\ & - \left\langle \boldsymbol{\theta}_2^\dagger(t+T) \mathcal{C}_2 \cdot \mathbf{u}_1 - \boldsymbol{\theta}_2^\dagger \cdot \mathcal{C}_0 \mathbf{u}_1(t-T) \right\rangle_2. \end{aligned}$$

Substituting this relation into (A7) gives

$$\begin{aligned} \partial_t \tau_2 \approx & \left\langle \partial_t \boldsymbol{\theta}_2^\dagger \cdot \mathbf{u}_1 + \boldsymbol{\theta}_2^\dagger \cdot \partial_t \mathbf{u}_1 \right\rangle_2 + \left\langle \boldsymbol{\theta}_2^\dagger(t+T) \mathcal{C}_2 \cdot \mathbf{u}_1 \right. \\ & \left. - \boldsymbol{\theta}_2^\dagger \cdot \mathcal{C}_0 \mathbf{u}_1(t-T) \right\rangle_2 - \left\langle \boldsymbol{\theta}_2^\dagger(t+T) \cdot (\mathcal{C}_2 - \mathcal{C}_0) \mathbf{u}_1 \right\rangle_2. \end{aligned}$$

Finally and integrating the full derivative $\partial_t (\boldsymbol{\theta}_2^\dagger \cdot \mathbf{u}_1)$ over the interval $[0, T_0/2]$ leads to

$$\begin{aligned} \partial_t \tau_2 \approx & \boldsymbol{\theta}_2^\dagger(T_0/2) \mathbf{u}_1(T_0/2) - \boldsymbol{\theta}_2^\dagger(0) \mathbf{u}_1(0) \\ & + \left\langle \boldsymbol{\theta}_2^\dagger(t+T) \cdot \mathcal{C}_0 \mathbf{u}_1 - \boldsymbol{\theta}_2^\dagger \mathcal{C}_0 \cdot \mathbf{u}_1(t-T) \right\rangle_2 \end{aligned} \quad (\text{A10})$$

Note that the only nonzero elements of the 4×4 matrix \mathcal{C}_0 are those within the 2×2 block with the elements having the indices $j, k \leq 2$. Hence, the last term in Eq. (A10)

$$\begin{aligned} & \left\langle \boldsymbol{\theta}_2^\dagger(t+T) \cdot \mathcal{C}_0 \mathbf{u}_1 - \boldsymbol{\theta}_2^\dagger \mathcal{C}_0 \cdot \mathbf{u}_1(t-T) \right\rangle_2 \\ & = - \left(\int_0^\delta + \int_{T/2}^{T/2+\delta} \right) \left[\boldsymbol{\theta}_2^\dagger(t+T) \mathcal{C}_0 \mathbf{u}_1 \right] dt \end{aligned} \quad (\text{A11})$$

contains only the asymptotical expressions for the field components, which are assumed to be small and are neglected in this study. Therefore, we can drop the last term in Eq. (A10).

The equation for slow evolution of τ_1 is derived in a similar way to Eq. (A10):

$$\begin{aligned} \partial_t \tau_1 \approx & \boldsymbol{\theta}_1^\dagger(0) \mathbf{u}_2(0) - \boldsymbol{\theta}_1^\dagger(T_0/2) \mathbf{u}_2(T_0/2) \\ & + \left\langle \boldsymbol{\theta}_1^\dagger(t+T) \cdot \mathcal{C}_0 \mathbf{u}_2 - \boldsymbol{\theta}_1^\dagger \mathcal{C}_0 \cdot \mathbf{u}_2(t-T) \right\rangle_1. \end{aligned} \quad (\text{A12})$$

Note, that the terms $\boldsymbol{\theta}_2^\dagger(T_0/2) \mathbf{u}_1(T_0/2)$ [$\boldsymbol{\theta}_1^\dagger(0) \mathbf{u}_2(0)$] can be neglected in (A10) [(A12)] due to the fast decay of the leading tail of the TCS solution and trailing edge of the adjoint neutral mode. The remaining terms $\boldsymbol{\theta}_2^\dagger(0) \mathbf{u}_1(0)$ [$\boldsymbol{\theta}_1^\dagger(T_0/2) \mathbf{u}_2(T_0/2)$] entering the Eq. (A10)

[(A12)] have very different magnitudes except for the case where the TCSs are close to be equidistant in the cavity, $\Delta\tau = \tau_2 - \tau_1 \approx \tau_0/2$. This means that except for this case the TCS interaction is strongly asymmetric and does not satisfy Newton's third law [4, 20, 21]. Thus, keeping only the second terms in the right hand sides of Eqs. (A10) and (A12) one gets for the time evolution

TCS time separation $\Delta\tau = \tau_2 - \tau_1$:

$$\partial_t \Delta\tau \approx \boldsymbol{\theta}_1^\dagger(T_0/2) \mathbf{u}_2(T_0/2) - \boldsymbol{\theta}_2^\dagger(0) \mathbf{u}_1(0). \quad (\text{A13})$$

The equation for the slow evolution of the phase difference $\Delta\phi = \phi_2 - \phi_1$ can be derived in a similar way. This equation reads:

$$\partial_t \Delta\phi \approx \boldsymbol{\varphi}_1^\dagger(T_0/2) \mathbf{u}_2(T_0/2) - \boldsymbol{\varphi}_2^\dagger(0) \mathbf{u}_1(0). \quad (\text{A14})$$

-
- [1] M. J. Ablowitz, T. P. Horikis, and S. D. Nixon. Soliton strings and interactions in mode-locked lasers. *Optics Communications*, 282(20):4127–4135, 2009.
- [2] N. Akhmediev, A. Ankiewicz, and J. Soto-Crespo. Multisoliton solutions of the complex ginzburg-landau equation. *Physical Review Letters*, 79(21):4047, 1997.
- [3] N. Akhmediev, A. S. Rodrigues, and G. E. Town. Interaction of dual-frequency pulses in passively mode-locked lasers. *Optics communications*, 187(4-6):419–426, 2001.
- [4] P. Camelin, J. Javaloyes, M. Marconi, and M. Giudici. Electrical addressing and temporal tweezing of localized pulses in passively-mode-locked semiconductor lasers. *Phys. Rev. A*, 94(6):063854, 2016.
- [5] P. Grelu and N. Akhmediev. Dissipative solitons for mode-locked lasers. *Nature photonics*, 6(2):84–92, 2012.
- [6] N. Guglielmi and E. Hairer. Implementing radau iia methods for stiff delay differential equations. *Computing*, 67(1):1–12, 2001.
- [7] A. Halanay. *Differential equations: Stability, oscillations, time lags*, volume 6. Elsevier, 1966.
- [8] T. Herr, V. Brasch, J. D. Jost, C. Y. Wang, N. M. Kondratiev, M. L. Gorodetsky, and T. J. Kippenberg. Temporal solitons in optical microresonators. *Nature Photonics*, 8(2):145–152, 2014.
- [9] T. J. Kippenberg, A. L. Gaeta, M. Lipson, and M. L. Gorodetsky. Dissipative Kerr solitons in optical microresonators. *Science*, 361(6402), 2018.
- [10] A. Kokhanovskiy, E. Kuprikov, and S. Kobtsev. Single- and multi-soliton generation in figure-eight mode-locked fibre laser with two active media. *Optics & Laser Technology*, 131:106422, 2020.
- [11] J. N. Kutz, B. Collings, K. Bergman, and W. Knox. Stabilized pulse spacing in soliton lasers due to gain depletion and recovery. *IEEE journal of quantum electronics*, 34(9):1749–1757, 1998.
- [12] B. A. Malomed. Bound states of envelope solitons. *Physical Review E*, 47(4):2874, 1993.
- [13] M. Marconi, J. Javaloyes, S. Balle, and M. Giudici. How lasing localized structures evolve out of passive mode locking. *Phys. Rev. Lett.*, 112(22):223901, Jun 2014.
- [14] L. Munsberg, J. Javaloyes, and S. V. Gurevich. Topological localized states in the time delayed adler model: Bifurcation analysis and interaction law. *Chaos: An Interdisciplinary Journal of Nonlinear Science*, 30(6):063137, 2020.
- [15] M. Nizette, D. Rachinskii, A. Vladimirov, and M. Wolfrum. Pulse interaction via gain and loss dynamics in passive mode locking. *Physica D: Nonlinear Phenomena*, 218(1):95–104, 2006.
- [16] D. Puzyrev, A. G. Vladimirov, A. Pimenov, S. V. Gurevich, and S. Yanchuk. Bound pulse trains in arrays of coupled spatially extended dynamical systems. *Phys. Rev. Lett.*, 119(16):163901, 2017.
- [17] J. M. Soto-Crespo and N. N. Akhmediev. Multi-soliton regime of pulse generation by lasers passively mode locked with a slow saturable absorber. *JOSA B*, 16(4):674–677, 1999.
- [18] M. Stöhr and M. Wolfrum. Temporal dissipative solitons in the morris–lecar model with time-delayed feedback. *Chaos: An Interdisciplinary Journal of Nonlinear Science*, 33(2):023117, 2023.
- [19] D. Turaev, A. G. Vladimirov, and S. Zelik. Long-range interaction and synchronization of oscillating dissipative solitons. *Physical Review Letters*, 108(26):263906, 2012.
- [20] A. G. Vladimirov. Short- and long-range temporal cavity soliton interaction in delay models of mode-locked lasers. *Physical Review E*, 105(4):044207, 2022.
- [21] A. G. Vladimirov, S. V. Gurevich, and M. Tlidi. Effect of cherenkov radiation on localized-state interaction. *Phys. Rev. A*, 97(1):013816, 2018.
- [22] A. G. Vladimirov, G. V. Khodova, and N. N. Rosanov. Stable bound states of one-dimensional autosolitons in a bistable laser. *Phys. Rev. E*, 63(5):056607, 2001.
- [23] A. G. Vladimirov, A. V. Kovalev, E. A. Viktorov, N. Rebrova, and G. Huyet. Dynamics of a class-A nonlinear mirror mode-locked laser. *Phys. Rev. E*, 100(1):012216, 2019.
- [24] A. G. Vladimirov, M. Tlidi, and M. Taki. Dissipative soliton interaction in kerr resonators with high-order dispersion. *Phys. Rev. A*, 103(6):063505, 2021.
- [25] A. G. Vladimirov and D. Turaev. New model for mode-locking in semiconductor lasers. *Radiophys. & Quant. Electron.*, 47(10-11):857–865, 2004.
- [26] A. G. Vladimirov and D. Turaev. Model for passive mode locking in semiconductor lasers. *Phys. Rev. A*, 72(3):033808, 2005.
- [27] A. G. Vladimirov, D. Turaev, and G. Kozyreff. Delay differential equations for mode-locked semiconductor lasers. *Opt. Lett.*, 29:1221–1223, 2004.
- [28] S. Yanchuk, S. Ruschel, J. Sieber, and M. Wolfrum. Temporal dissipative solitons in time-delay feedback systems. *Phys. Rev. Lett.*, 123(5):053901, 2019.
- [29] A. Zaviyalov, P. Grelu, and F. Lederer. Impact of slow gain dynamics on soliton molecules in mode-locked fiber lasers. *Optics letters*, 37(2):175–177, 2012.